Accurate bacterial outbreak tracing with Oxford Nanopore sequencing and reduction of methylation-induced errors

Mara Lohde[1], Gabriel E. Wagner[5], Johanna Dabernig-Heinz[5], Adrian Viehweger[4], Sascha D. Braun[2,3], Stefan Monecke[2,3], Celia Diezel[2,3], Claudia Stein[1], Mike Marquet[1], Ralf Ehricht[2,3,6], Mathias W. Pletz[1,2] and Christian Brandt[1,2]

[1] Institute for Infectious Diseases and Infection Control, Jena University Hospital, Jena, Germany
[2] InfectoGnostics Research Campus, Centre for Applied Research, Jena, Germany
[3] Leibniz-Institute of Photonic Technology (Leibniz-IPHT), Jena, Germany
[4] Institute of Medical Microbiology and Virology, University Hospital Leipzig, Leipzig, Germany
[5] Diagnostic and Research Institute of Hygiene, Microbiology and Environmental Medicine, Medical University of Graz, Graz, Austria
[6] Institute of Physical Chemistry, Friedrich-Schiller-University Jena, Jena, Germany

Abstract

Our study investigated the effectiveness of Oxford Nanopore Technologies for accurate outbreak tracing by resequencing 33 isolates of a three-year-long *Klebsiella pneumoniae* outbreak with Illumina short read sequencing data as the point of reference.

We detected considerable base errors through cgMLST and phylogenetic analysis of genomes sequenced with Oxford Nanopore Technologies, leading to the false exclusion of some outbreak-related strains from the outbreak cluster. Nearby methylation sites cause these errors and can also be found in other species besides *K. pneumoniae*. Based on this data, we explored PCR-based sequencing and a masking strategy, which both successfully addressed these inaccuracies and ensured accurate outbreak tracing. We offer our masking strategy as a bioinformatic workflow (MPOA is freely available on GitHub under the GNUv3 license: github.com/replikation/MPOA) to identify and mask problematic genome positions in a reference-free manner.

Our research highlights limitations in using Oxford Nanopore Technologies for sequencing prokaryotic organisms, especially for investing outbreaks. For time-critical projects that cannot wait for further technological developments by Oxford Nanopore Technologies, our study recommends either PCR-based sequencing or using our provided bioinformatic workflow. We would advise that read mapping-based quality control of genomes should be provided when publishing results.

Keywords

Klebsiella pneumoniae, Whole Genome Sequencing, cgMLST, Phylogenetic analysis, erroneous basecalling, LRS Special Issue

Introduction

Whole genome sequencing is essential for analyzing outbreaks, pandemics, or phylogenetic relationships (Wyres et al. 2020; Chewapreecha et al. 2017). The recent SARS-CoV-2 pandemic has thus led to a leap in the integration and expansion of sequencing capacities in many laboratories and hospitals, predominantly using Illumina for short-read sequencing or Oxford Nanopore Technologies (ONT) for long-read sequencing (approx. 78% and 18%, respectively) (Brandt et al. 2021). Beyond viral pandemic tracking, bacterial pathogen outbreaks, particularly those linked to antibiotic resistance, continue to impose a significant global public health burden (Murray et al. 2022). Gram-negative bacteria, in particular, rapidly acquire antibiotic resistance via horizontal gene transfer from other species (Moura de Sousa et al. 2023; Hadjadj et al. 2022; Lerminiaux and Cameron 2019). This mechanism complicates tracking outbreaks or identifying their origin, as a single specific plasmid or mobile element can be responsible for a persistent outbreak or multiple outbreaks across unrelated species (Hadjadj et al. 2022; Abe et al. 2021; Sivertsen et al. 2014; Pletz et al. 2018). Additionally, in gram-negative bacteria, DNA methylation plays a crucial role in epigenetic regulation, which impacts gene expression, genome modification, virulence, mismatch repair, and other physiological activities (Gao et al. 2023; Wang et al. 2023).

Effectively tracking these complex molecular mechanisms requires careful strategic monitoring and sequencing-based investigation. Consequently, the accuracy and continuity of the genome data are paramount. Illumina, a short-read sequencing method with an error rate of less than 0.8% in raw data, is frequently used as its complementary genome reconstruction precision exceeds 99.997% (Wang et al. 2021). However, repetitive elements, such as transposons, present a substantial challenge for short reads when reconstructing closed bacterial genomes and their accompanying plasmids. Long-read sequencing technologies like Pacific Bioscience (PacBio) and Oxford Nanopore Technologies can resolve such elements, e.g. plasmids, as they achieve longer read lengths averaging around

10-20 kb and even up to 3.85 Mb in the case of ONT (Dohm et al. 2020; Eid et al. 2009; Tyson et al. 2018; Grohme et al. 2018).

Real-time sequencing allows data collection and analysis, while sequencing positions Oxford Nanopore Technologies as an appealing choice for hospital surveillance and outbreak control (Spott et al. 2022). Owing to their recently launched flow cells (R10.4.1) and chemistry (SQK-NBD114.24), they have achieved raw read accuracy that now exceeds 99.1% (Ni et al. 2023). Several studies have shared their findings and reported accuracy levels similar to those from short-read data (Wagner et al. 2023; Sanderson et al. 2023). However, significant discrepancies between Illumina and ONT genomes were also observed for some organisms (Linde et al. 2023).

These contradictions can lead to inaccurate conclusions, like excluding outbreak-associated samples when investigating outbreaks. In addition, genomes are usually stored in open public databases such as NCBI or ENA, which can lead to error propagation and potentially significantly affect patients' welfare. Therefore, we used ONT to reevaluate a well-documented, three-year-long outbreak initially analyzed with Illumina data to address these contradictory statements, focusing on the errors in ONT sequencing data (Viehweger et al. 2021). *K. pneumoniae* is an ideal microorganism for this topic, as it is a common pathogen linked to hospital-wide outbreaks carrying plasmids with multidrug resistance genes (Brandt et al. 2019). When using ONT-only data, we identified a few critical issues leading to erroneous basecalls for *K. pneumoniae*. We noticed similar problems and clear patterns in other organisms, which need to be considered during outbreak identification, even though we could resolve them.

Results

Erroneous basecalls occur in some strains but not others and vary by basecaller and sequencing kits

We resequenced the genomes of 33 randomly distributed *K. pneumoniae* samples isolated from 31 patients (from a total of 114 outbreak-related isolates) using R10.4 and R10.4.1 flow cells, along with the corresponding library preparation kits (henceforth “Kit 12”: SQK-NBD112.24 (early access) and “Kit 14”: SQK-NBD114.24 (successor)). Our objective was to investigate whether previously reported conflicting statements could be replicated (Wagner et al. 2023; Sanderson et al. 2023; Linde et al. 2023). We used core genome multilocus sequence typing (cgMLST) to compare ONT and Illumina-sequenced genomes. The comparison of the 33 samples revealed 11 outliers in the ONT data, showing high allelic deviations (up to 46) to their short-read counterparts while not matching the outbreak cluster (Supplementary Figure 1 and 2). While the remaining samples closely match the outbreak cluster, the outliers highlight inconsistencies within the ONT data, as reported in the literature. To assess whether either the basecaller or their models might be responsible, we re-basecalled and compared an outlier sample (UR2602) in detail to three samples, where we assume error-free genomes based on cgMLST (Figure 1; see method section “Basecalling and Assembly” for further details) and pairwise SNP calling (Supplementary Figure 3) with Illumina genomes.

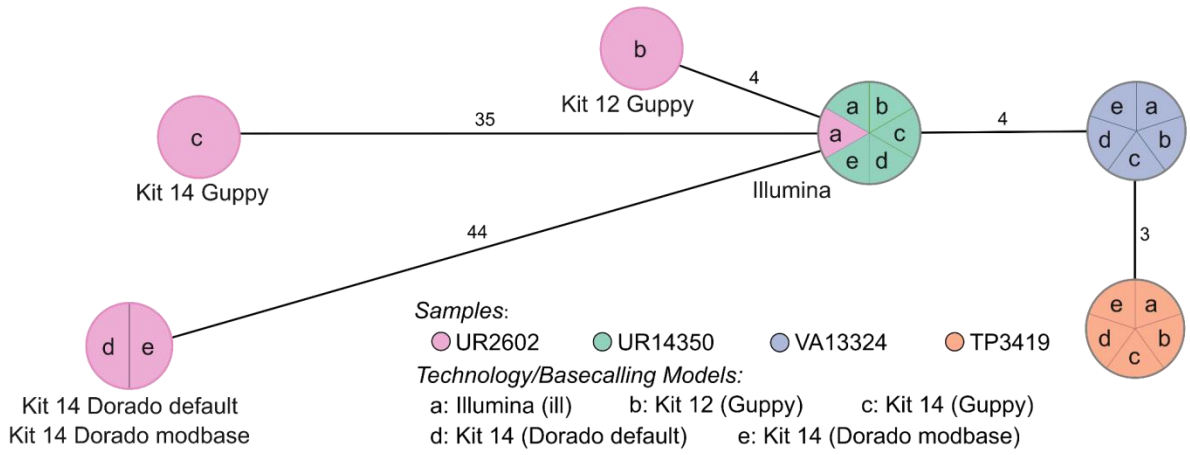

Figure 1: cgMLST typing reveals allelic differences between genomes utilizing different basecaller and models, and sequencing kits. The minimum spanning tree pictures four *K. pneumoniae* samples based on 2,358 genes for pairwise comparison of allelic variations. Missing values were ignored. Nodes (samples) are connected by lines depicting the distance by numbers of allelic differences. Loci are considered different if one or more bases change between the samples. Loci without allelic differences are described as being the same. Samples with allelic differences ≤15 are considered as part of the cluster. All isolates were prepared with Kit 14 and Kit 12 and basecalled with each respective Guppy "super accurate" basecalling model (see methods "Basecalling and Assembly"). We basecalled all Kit 14 - prepared samples with Dorado using the default and a modification-aware model (see methods "Basecalling and Assembly").

Based on 2,358 loci for the cgMLST, no allelic differences, regardless of kit, basecaller, or basecaller model, were identified for the isolates UR14350, VA13324, and TP3419. In contrast, the outlier sample (UR2602) revealed allelic variations for each kit, basecaller, and sequencing technology. Despite both basecallers using the same raw signal data, the 35 allelic variations in Guppy differ without accordance from the 44 allelic variations in Dorado.

By cgMLST, the outlier sample prepared with Kit 14 would be falsely assigned as not part of the outbreak due to its 35 or 44 allelic differences, even though the sample exhibits low allelic differences according to the short-read data (gold standard). Conversely, when

126 prepared with early access Kit 12, the same isolate would be correctly considered as only
127 four different loci could be observed (adhering to the recommended allelic difference cut-off
128 of ≤15) (Miro et al. 2020). Since the basecalling models disagreed on the allelic differences,
129 we suspected more issues within the raw data (reads and raw signals) and conducted a
130 comprehensive analysis of all possible affected positions.

131 Ambiguities in purine or pyrimidine discrimination for a subset 132 of genome positions can cause erroneous basecalls

133 The first visual inspection of mapped reads to the assembly revealed read ambiguity on
134 certain positions indicated by varying base ratios (ambiguous positions). For further
135 characterization of these ambiguous positions, we examined our data on the sequence,
136 nucleotide, and raw signal level (Figure 2). For each ambiguous position on the
137 chromosomal DNA for 33 *K. pneumoniae* outbreak samples, we determined the ratio
138 between the two bases by counting their occurrences for both strand orientations within the
139 read data at that position (Figure 2 A). Searching for characteristic “indicator” sequence
140 motifs, we explored the surrounding base for each detected ambiguous position and plotted
141 the observed pattern as a sequence logo (Figure 2 B and Supplementary Table 1).
142 Additionally, we compared the methylated and unmethylated raw signals around these
143 ambiguous positions (Figure 2 C).

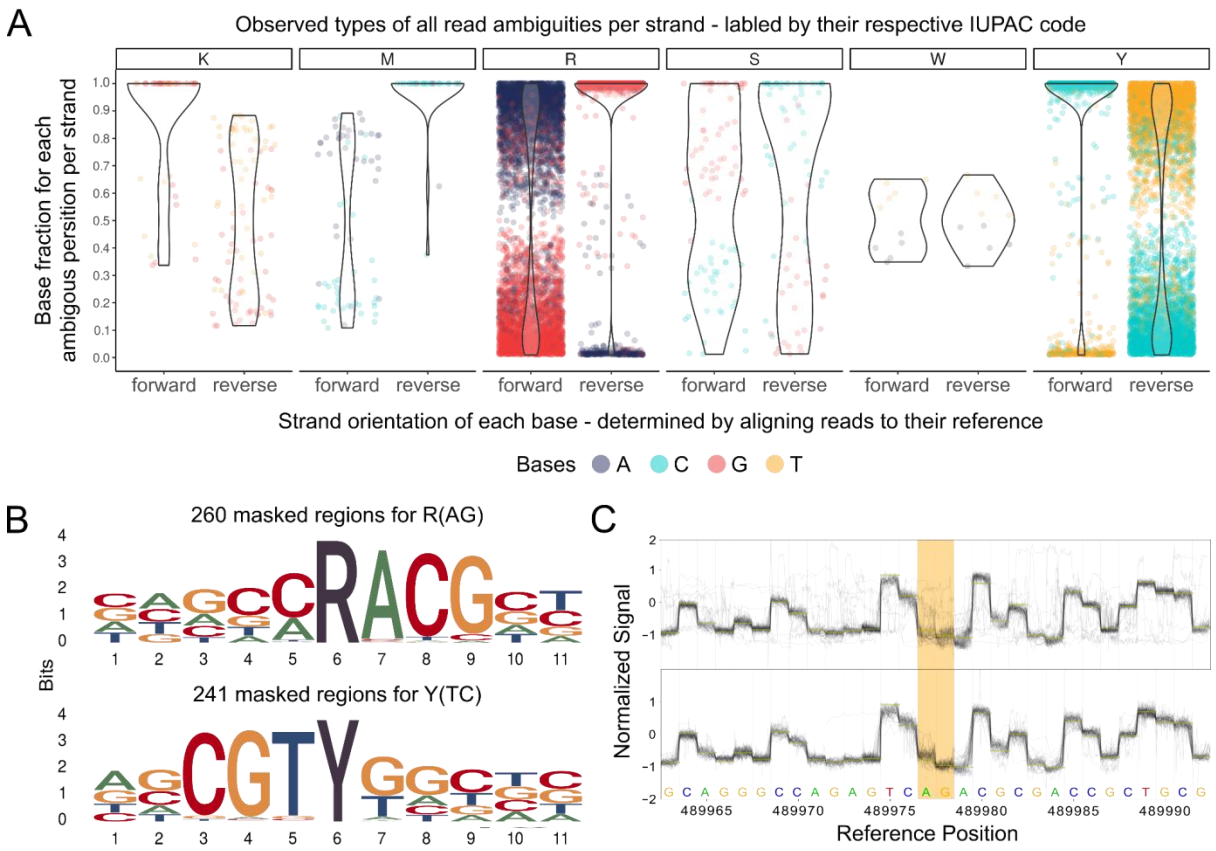

Figure 2: Systematic examination of ambiguous positions for frequency by strand orientation (A), conserved sequences (B), and raw Nanopore signal (C). A: Violin chart showing the ratio between two bases within the mapped read data separated by strand orientation for 6,556 ambiguous positions in 33 *K. pneumoniae* samples. Every ambiguous position is divided by which two bases appear and labeled by their respective degenerative base (IUPAC nucleotide code). For example, "R" stands for a combination where either A or G is found at that position. Each dot represents a base occurrence within the respective base combination at the ambiguous position. **B:** Sequence logo of observed sequence pattern around the ambiguous bases R and Y on the chromosomal contig of *K. pneumoniae* for one sample. **C:** Raw signal level (FAST5/POD5) of ambiguous positions (yellow) for Kit 14 (above) with methylated bases and SQK-RPB114.24 without modifications (below). Less clear signals are observable in ambiguous positions (yellow) for Kit 14. Signal plots were generated with remora (v.2.1.3; github.com/nanoporetech/remora).

158 As highlighted in Figure 2 A, in some positions, the basecaller can not determine between
159 either of two bases, expressed by specific base ratios varying per position and strand
160 orientation, resulting in erroneous assemblies. We could not observe ambiguous positions
161 containing more than two different bases. For clarity, we assign the IPUAC nucleotide code
162 for degenerate bases (R, Y, M, K, S, W) to each ambiguous position varying between two
163 bases. Accordingly, we will refer, e.g. to "R" when the positions contain A or G in the read
164 data.

165 Out of our analysis of 33 *K. pneumoniae* outbreak isolates, we discovered 6,556 positions
166 that exhibit ambiguity (Figure 2A). The ambiguity mainly resolved around 3,311 positions for
167 R and 3,111 for Y. In 5,442 of 6,455 R and Y positions (84.31%), the basecalled reads lean
168 towards Cytosine or Guanine (C or G). We detected other ambiguous positions in K (44), M
169 (34), S (51), and W (5), but with comparable lower occurences. It is essential to
170 acknowledge that not all identified ambiguous positions result in errors in the assembled
171 genome, which explains the varying error profile of the same sample (Figure 1). Errors in
172 these ambiguous positions mainly arise when deciding between purine bases (A or G) or
173 pyrimidine bases (T or C). Since strand bias is reported as a substantial factor for false
174 positive variant detection, we considered the strand orientation of the read data
175 (Leija-Salazar et al. 2019). In most cases, we noticed that the correct base is located clearly
176 and more frequently on both strand orientations, while the incorrect base is less prevalent.
177 For instance, the correct base Guanine is found on both strands for positions masked by R
178 and is predominantly found on the reverse strand (Fig 2 A: see R reverse), less frequently on
179 the forward strand, which also contains the false base. We detected similar behavior for
180 other species (Supplementary Figure 6).

181 In the error-prone genomes of the *K. pneumoniae* outbreak, we detected preserved patterns
182 around the ambiguous positions R and Y (Figure 2B). These sequence motifs are reverse-
183 complement patterns (RACG/CGTY), pointing to a singular issue. Compared to other

184 isolates of *K. pneumoniae*, we also observed additional patterns. These motifs are likely
185 specific to particular strains.

186 Furthermore, we examined and collected additional ONT sequencing data that used the Kit
187 14 library preparation (264 isolates across 32 species) to investigate whether the ambiguous
188 positions are *K. pneumoniae* exclusive (Table 1). These samples were collected based
189 solely on Kit 14 library preparations and not on whether they were associated with an
190 outbreak. Compared to all other species samples, we determine the fewest ambiguous
191 positions (0 to 1) in *Bordetella pertussis*. In contrast, all 10 *Enterococcus faecalis* isolates
192 had over 200 ambiguous positions. Over 40% of 264 screened samples have more than 50
193 ambiguous positions. Across all species, the minimal shared sequence motif was RA/TY.
194 Certain species, such as *Acinetobacter junii*, *Acinetobacter radioresistens*,
195 *Chryseobacterium gleum*, *Enterobacter cloacae*, *Micrococcus luteus,* and
196 *Stenotrophomonas maltophilia*, exhibited a considerable number of ambiguous positions.
197 This suggests that many species may be impacted, but not necessarily all strains.
198

199 As methylated bases are probably liable for ambiguous positions, we compared sequencing
200 data with methylations (Kit 14) (Figure 2 C above) and without (SQK-RPB114.24) (Figure 2
201 C below) on the raw signal level from FAST5/POD5 files before basecalling occurs. We
202 choose the raw signal level for investigation prior to any bioinformatic approaches (e.g.,
203 basecalling, assembly, polishing) to avoid the potential introduction of other biases or errors.
204 For native sequencing, less clear signals at these positions are observable, which might
205 cause these ambiguous basecalls. These noisy signals could explain the frequencies of
206 bases we detected in the reads (Figure 2A) and, thus, the basecaller's difficulty in deciding
207 on a specific base for that position.
208

209 We found no coherent methylation motifs in the literature that would fit the observed pattern.
210 Nevertheless, it has been reported that methylated bases can affect the raw signal in the

211 surrounding region (Tourancheau et al. 2021). Thus, we can not determine whether multiple
212 methylation motifs are the cause or if an unknown motif is present. Accordingly, to these
213 findings, we evaluated whether PCR-based sequencing or a bioinformatic masking strategy
214 for ambiguous positions can reliably remove these methylation-based errors for outbreak
215 analysis.

216 **Table 1:** Overview of R (A-G) and Y (T-C) base ambiguity for 264 isolates from 32 various species, sequenced with Oxford Nanopore
217 Technologies using Kit 14. Only chromosomal contigs were analyzed, and only "super accurate" basecalling models were used. Chromosomes
218 were coverage-masked by N if below a read depth of 10x. N positions were not considered for the table to avoid overestimating one base
219 ambiguity.

Species	Total samples	Samples with > 50 ambig. P.	Mean R (A-G) ambiguity per sample (min/max)	Mean Y (T-C) ambiguity per sample (min/max)	Motif type	Reference
Achromobacter xylosoxidans	1	0 (0%)	6	4	NA	*
Acinetobacter baumannii	15	5 (33.33%)	22.53 (0/109)	19.87 (0/83)	NA	*
Acinetobacter junii	1	1 (100%)	279	223	CA**R**ATG CAT**Y**TG	*
Acinetobacter mesopotamicus	1	1 (100%)	53	28	NA	*
Acinetobacter radioresistens	1	1 (100%)	175	150	**R**A T**Y**	*
Acinetobacter soli	1	0 (0%)	12	11	NA	*

Bordetella pertussis§	40	0 (0%)	0.1 (0/1)	0.2 (0/1)	NA	(Wagner et al. 2023)
Chryseobacterium arthrosphaerae	1	0 (0%)	13	7	NA	*
Chryseobacterium gleum	1	1 (100%)	218	217	**R**ACGC GCGT**Y**	*
Citrobacter freundii	3	3 (100%)	145.67 (49/329)	137.67 (39/319)	C**R**ATGTC GACAT**Y**G	*
Citrobacter portucalensis	2	2 (100%)	29 (26/32)	29 (28/30)	**R**A T**Y**	*
Enterobacter cloacae	1	1 (100%)	153	162	NA	*
Enterobacter hormaechei	5	1 (20%)	15.60 (4/45)	15.60 (6/42)	NA	*
Enterococcus faecalis	10	10 (100%)	250.40 (223/275)	249.00 (210/270)	T**R**AG CT**Y**A	+
Enterococcus faecium	19	2 (10.53%)	15.74 (0/27)	14.63 (0/28)	**R**ACC GGT**Y**	#
Escherichia coli	8	3 (37.50%)	31.38 (2/118)	29.31 (4/111)	NA	*

Escherichia flexneri	10	9 (90%)	49.10 (19/88)	44.70 (18/88)	**R**AT ATY	*
Klebsiella aerogenes	1	0 (0%)	22	17	NA	*
Klebsiella michiganensis	1	1 (100%)	56	42	NA	*
Klebsiella pneumoniae	70	38 (54.29%)	97.04 (3/835)	92.47 (3/847)	**R**ACG CGT**Y**	(Viehweger et al. 2021) * #
Klebsiella oxytoca	1	0 (0%)	5	9	NA	*
Listeria monocytogenes	17	3 (17.65%)	37.94 (0/514)	40.82 (0/557)	NA	#
Micrococcus luteus	1	1 (100%)	172	220	C**R**AC GT**Y**G	*
Proteus mirabilis	1	1 (100%)	45	43	C**R**AC GT**Y**G	*
Pseudomonas aeruginosa	19	6 (33.33%)	389.17 (0/2251)	387.56 (0/2290)	AA**R**ACC GGT**Y**TT	*

Pseudomonas asiatica	2	1 (50%)	145 (0/290)	144.50 (0/289)	CC**R**A T**Y**GG	*
Pseudomonas stutzeri	1	0 (0%)	14	16	NA	*
Salmonella enterica	2	1 (50%)	41.5 (7/76)	42.5 (7/78)	NA	*
Stenotrophomonas maltophilia	1	1 (100%)	229	171	TAC**R**AC GT**Y**GTA	*
Serratia marcescens	4	4 (100%)	107.75 (68/178)	99.5 (67/171)	CC**R**A T**Y**GG	*
Shewanella algae	2	2 (100%)	71.5 (37/106)	50 (32/68)	NA	*
Staphylococcus aureus	20	8 (40%)	23.35 (0/99)	23.35 (0/97)	**R**ACC GGT**Y**	#

220 * Sequenced strains received from Leibniz-Institute of Photonic Technology, Optisch-Molekulare Diagnostik und Systemtechnologie
221 # Diagnostic and Research Institute of Hygiene, Microbiology and Environmental Medicine, Medical University of Graz
222 + Own samples from the Jena University Hospital
223 § Sequenced with Kit 12, resequencing via Kit 14, showed no differences

Strategies to mitigate methylation-induced basecalling errors

To solve methylation-induced basecalling errors in ambiguous base positions, we evaluated two strategies: 1) We resequenced 10 *K. pneumoniae* outbreak samples using the Nanopore Rapid PCR Barcoding Kit (SQK-RPB114.24) to remove methylated bases prior to sequencing and analyzed the genomes using cgMLST and phylogenetic analysis (Figure 3 A and B). 2) We masked ambiguous positions for Kit 14 prepared genomes with our bioinformatic workflow (see method section “Workflow for detecting and masking of ambiguous positions”). It is important to mention that these masked assemblies cannot be used for cgMLST because allelic differences cannot be accurately determined for genes with masked bases. Therefore, the masked genomes were only used for phylogenetic analysis (Figure 3 B). Furthermore, it should be noted that cgMLST only considers coding sequences, whereas the phylogenetic analysis assesses the entire genome that is represented in all samples, which gives a higher resolution for base differences.

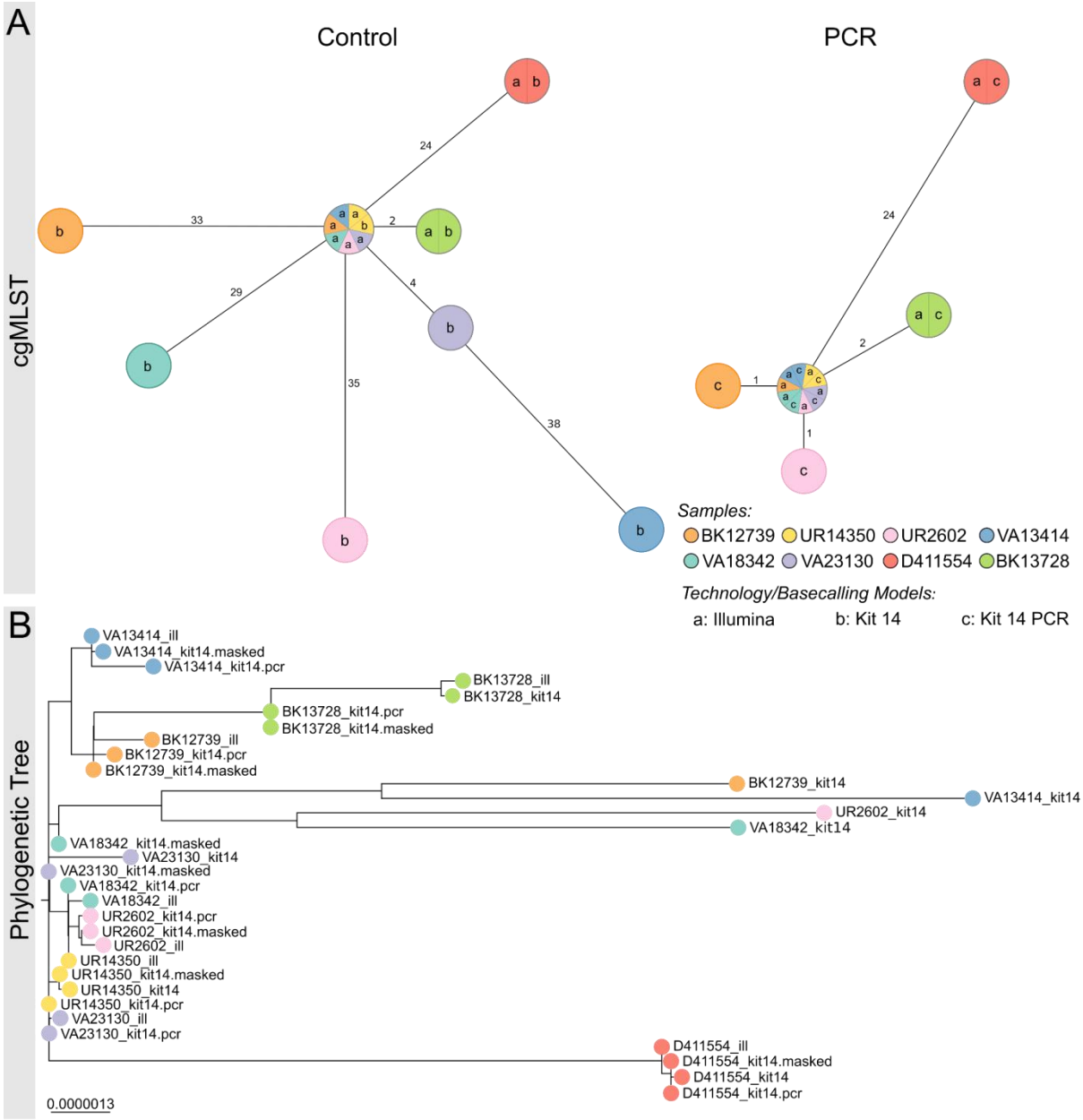

Figure 3: PCR-based sequencing or masking of ambiguous positions reduces allelic or phylogenetic distances. A: Minimum spanning trees (pairwise ignore missing values) of each of eight *K. pneumoniae* outbreak samples based on 2,358 genes to compare allelic differences between Illumina and Nanopore SQK-NBD114.24 genomes (kit14; left) and Illumina and Nanopore SQK-RPB114.24 genomes (PCR; right). Nodes (samples) are connected by lines depicting the distance by numbers of allelic differences. Loci are considered different whether one or more bases change between the samples. Loci without allelic differences are described as being the same. Samples with allelic differences ≤15 are considered as part of the cluster. **B:** Phylogenetic tree based on core genome SNP

247 alignment between eight *K. pneumoniae* outbreak samples (colored nodes), prepared with
248 Illumina (ill), Nanopore SQK-NBD114.24 (kit14) and SQK-RPB114.24 (pcr) compared to the
249 masked Kit 14 assemblies (masked).

250 When comparing the Native Barcoding with the PCR-based Kit, ambiguous positions were
251 significantly reduced from 2,316 to just 14 for R and Y across the 10 resequenced *K.*
252 *pneumoniae* samples (Supplementary Table 2). Both the minimum spanning trees and the
253 phylogenetic tree also show this significant improvement in genome quality for ONT (Figure
254 3). According to the cgMLST, the outlier samples UR2602 and BK12739 now closely match
255 the Illumina genome, down to only one allele difference from 35/33 (Figure 3 A). When
256 comparing phylogenetic distances within the phylogenetic tree, an increased convergence
257 with the Ilumina genomes, particularly for the outlier samples, was observed, too (Figure 3
258 B). Additionally, masked and PCR-based assemblies have almost no phylogenetic
259 divergence.

260 Further, we analyzed the phylogenetic tree containing native Kit 14, masked native Kit 14,
261 and Illumina genomes for all 33 *K. pneumoniae* samples (Supplementary Figure 4). These
262 include 11 Kit 14 outliers (average of 492 ambiguous positions) and 22 Kit 14 genomes with
263 an average of less than 52 ambiguous positions. We observed two types of phylogenic
264 distances between ONT Kit 14 and Illumina: The expected considerable distances between
265 the outlier and Illumina genomes are due to ambiguity and, in some cases, a phylogenetic
266 distance for which ambiguity is not the causation.

267 By masking ambiguous bases, we observed that 8 of 11 outlier genomes now closely align
268 with their respective Illumina genome. The remaining three outlier samples changed their
269 tree positions after masking, now closely aligning with other Illumina genomes but still
270 diverged from their corresponding Illumina genome due to other non-ambiguity-related
271 differences. For the other 22 masked Kit 14 genomes with less ambiguity than the outliers,

272 we did not observe any substantial changes in their tree positions, as fewer positions were
273 masked.

274 In summary, 22 out of 33 masked ONT genomes align with their respective Illumina
275 genomes, and the remaining 11 do not. In these cases, the remaining distances do not result
276 from ambiguous positions within the ONT assemblies. For instance, the Illumina and ONT
277 genomes of TP3870 matched perfectly in the minimum spanning tree, but they exhibited
278 some distance from each other in the phylogenetic tree (Supplementary Figure 4). We
279 identified reconstruction issues in these short-read assemblies, primarily manifesting in non-
280 coding regions (Supplementary Figure 5). Since cgMLST only compares coding sequences,
281 these errors do not affect the result analysis. Therefore, we recommend using only one
282 technology when performing whole genome comparison for outbreak analysis.

Discussion

Over the past few years, Oxford Nanopore Technologies has been effectively used to monitor and track the SARS-CoV-2 pandemic and its viral lineages. Despite this, contradictory reports have emerged regarding the consistency of ONT-sequenced bacterial genomes compared to Illumina-based. Our research examined whether Oxford Nanopore Technology can be used to analyze bacterial outbreaks accurately.

For our investigation, we resequenced a well-documented 3-year *K. pneumoniae* outbreak using the Nanopore Native Barcoding Kit 14 for library preparation. Our analyses demonstrated that the raw signals were impacted by methylated bases, creating ambiguous positions through basecalling and leading to erroneous exclusions of certain outbreak-associated strains. However, not all isolates are affected by these ambiguities, and none or minimal allelic differences are shown in the corresponding short-read data. One should note that some errors in non-coding areas for Illumina assemblies were observed, which can lead to higher distances within a phylogenetic tree but with little to no effect in cgMLST. Despite focusing on *K. pneumoniae* initially, other prokaryotic organisms are also impacted. Crucially, we also detected ambiguous positions using the predecessor sequencing Kit SQK-LSK109 (Supplementary Table 3). Consequently, when using ONT-based sequence data from open public databases or when analyzing outbreaks, test for read ambiguity by using e.g. the provided MPOA workflow before further analysis.

Based on our in-depth investigation, we recommend using the Nanopore Rapid PCR Barcoding Kit for sequencing to eliminate these read ambiguities in the genome assemblies. However, this method decreases the read length to roughly 3,500 bp, posing difficulties in achieving closed plasmids and genomes, similar to other short-read approaches but to a way lesser extent. A higher sequencing depth might also be necessary to control for polymerase errors. For samples already sequenced without any involvement of PCR, we propose using the provided MPOA workflow to assess the quality of each genome. This

309 workflow offers information about the frequency and strand orientation of reads in
310 ambiguous positions and masks them in the assembly by the IUPAC nucleotide code without
311 needing another reference. These masked assemblies can be used for constructing
312 phylogenetic trees for outbreak tracking. However, cgMLST cannot be performed as masked
313 or degenerated bases create false allelic differences across the whole minimal spanning tree.

314 Given the notable strides made in direct methylation calling techniques, Oxford Nanopore
315 Technology might overcome the issues with ambiguous positions. If available in high enough
316 quantities, duplex reads (connecting and sequencing both strands) might provide better raw
317 signal data for accurate basecalling. The recently introduced research model reduces the
318 ambiguous positions in direct comparison, but still a few remain (Supplementary Table 4;
319 Researchmodel "res_dna_r10.4.1_e8.2_400bps_sup" available on
320 github.com/nanoporetech/rerio, not yet implemented in MinKnow version 23.07.12, as of
321 30.11.2023). Further advances that reduce methylation-induced errors for certain specific
322 motifs are being developed, as shown for *Listeria monocytogenes* and *Escherichia coli*
323 (Chiou et al. 2023; Hallgren et al. 2021). Nevertheless, we strongly recommend constantly
324 testing and evaluating reconstructed prokaryotic genomes to avoid erroneous conclusions
325 based on these ambiguous positions introduced by unknown and not yet considered
326 methylation motifs.

Methods

Isolates and Genomic Data

Oxford Nanopore Technologies sequencing data from three institutes have been collected and analyzed. The sequencing data includes 264 isolates from 32 species, provided by the Leibniz-Institute of Photonic Technology Jena, Medical University of Graz, and University Hospital Jena. Additionally, a set of 80 samples containing *K. pneumoniae*, *E. faeces*, *L. monocytogenes*, *and Staphylococcus aureus* from a ring trail were used for analysis. University Hospital Leipzig provided 33 Carbapenem-resistant *K. pneumoniae* outbreak isolates from sequence type 258 and the associated Illumina sequencing data (Supplementary Table 5). We ensured these samples were scattered across the whole phylogenetic tree that Viehweger et al. provided in their manuscript.

Genomic DNA Isolation

Isolates from 10% glycerin cryo culture streaked out on Columbia Agar with 5% Sheep Blood (Becton Dickinson). After overnight incubation, a single colony was selected and cultured overnight in MH-Broth. Genomic DNA was isolated via ZymoBIOMICS DNA Microprep Kit (D4301 and D4305; ZymoResearch) with modifications to enhance the output yield. Qubit dsDNA BR Assay-Kit (Thermo Fisher Scientific) was employed to quantify DNA concentrations from each sample. This kit uses fluorescent dyes to measure double-stranded DNA to ensure reliable results.

Whole Genome Sequencing

To prepare the library for sequencing using Oxford Nanopore Technologies' GridION system, we used the Native Barcoding Kit 24 V12 (SQK-NBD112.24, Oxford Nanopore Technologies) and Native Barcoding Kit 24 V14 (SQK-NBD114.24, Oxford Nanopore Technologies) with

350 R10.4 and R10.4.1 flow cells, respectively. Both sequencing protocols were optimized
351 regarding prolonged incubation times. Additionally, one library was prepared with Rapid PCR
352 Barcoding Kit 24 (SQK-RPB114.24, Oxford Nanopore Technologies) for sequencing on an
353 R10.4.1 flow cell. Sequencing of libraries prepared with SQK-NBD112.24 and SQK-
354 NBD114.24 was conducted at 4kHz with 260bps, while SQK-RPB114.24 was conducted at
355 5kHz with 400bps. The DNA fragments minimum length for all sequencing runs was set to
356 200bp in MinKNOW (v22.12.5) software.

357 Basecalling and Assembly

358 Basecalling and barcode demultiplexing of long-read sequencing data was performed on the
359 GridiION (Oxford Nanopore Technologies) deploying Guppy (v6.4.6) using super accurate
360 models associated with the different used sequencing kits ("dna_r10.4_e8.1_sup.cfg",
361 "dna_r10.4.1_e8.2_260bps_sup.cfg", "dna_r10.4.1_e8.2_5khz_400bps_sup.cfg"). For
362 further analysis, Dorado (v0.3.0) was used ("dna_r10.4.1_e8.2_260bps_sup.cfg" and
363 "dna_r10.4.1_e8.2_260bps_modbases_5mc_cg_sup.cfg").
364 Reads were filtered by excluding them below 1,000bp with Filtlong (v.0.2.1)
365 (https://github.com/rrwick/Filtlong). *De novo* assembly was conducted using Flye (--meta --
366 nano-hq) (v2.9) (Kolmogorov et al. 2019). Filtered reads were mapped to the assembly using
367 Minimap2 (-ax map-ont) (v2.18) (Li 2018) and polished afterward by Racon (v1.4.20;
368 github.com/lbcb-sci/racon) followed by medaka_consensus polishing both in default settings
369 (v1.5.0; github.com/nanoporetech/medaka) using the following models:
370 *r104_e81_sup_g5015*, *dna_r10.4.1_e8.2_260bps_sup@v3.5.2*,
371 *r1041_e82_260bps_sup_g632* (Supplementary Code 1). Short reads obtained by Illumina
372 sequencing were assembled using Shovill (v1.1.0, github.com/tseemann/shovill), which
373 includes various genome corrections and polishing approaches (Viehweger et al. 2021).

374 ## Core genome multilocus sequence typing of *K. pneumonia*

375 For core genome multilocus sequence typing (cgMLST), we used a species-specific public
376 cgMLST scheme for a gene-by-gene comparison on an allelic level (Mellmann et al. 2016;
377 Leopold et al. 2014) according to the '*K. pneumoniae sensu lato* cgMLST'
378 (https://www.cgmlst.org/ncs/schema/2187931/). This comprises a total of 2358 genes (about
379 40% of the NTUH-K2044 reference genome) (Bialek-Davenet et al. 2014) in flye-assembled
380 and polished long-read and Shovill-assembled short-read assemblies (v1.1.0,
381 github.com/tseemann/shovill). To illustrate the clonal relationships between different isolates,
382 a minimum-spanning tree analysis was performed based on the determined allelic profiles
383 using the Ridom SeqSphere^{+} software version 7 (Ridom GmbH, Muenster, Germany)
384 (Jünemann et al. 2013) with the parameter "pairwise ignore missing values". We defined a
385 clonal transmission event if the isolates differ ≤15 alleles for *K. pneumoniae* (Miro et al.
386 2020).

387 ## Phylogenetic tree

388 The phylogenetic trees visualize the evolutionary relationship among *K. pneumoniae*
389 outbreak strains and are constructed based on core genome SNP alignment using Snippy-
390 core (v4.6.0; github.com/tseemann/snippy). The phylogenetic tree was built using FastTree
391 (Price et al. 2009) and visualized in Microreact (Argimón et al. 2016).

392 ## Workflow for detection and masking of ambiguous positions

393 We developed a standardized Nextflow (Di Tommaso et al. 2017) workflow for *de novo*
394 quality validation of all species, which is publicly available at github.com/replikation/MPOA,
395 licensed under GNU General Public License v3.0. The workflow only needs the genome file
396 (FASTA) and the associated reads (FASTQ) (Figure 4). The workflow provides reproducible
397 quality control by counting and summarizing ambiguous bases for the user, masking low

398 coverage regions (0-10x depth) with BEDTools (Quinlan and Hall 2010) (v2.31.0), and
399 providing an assembly with these positions masked by the IUPAC nucleotide code for
400 subsequent analysis. The workflow utilizes Docker or singularity container and is compatible
401 with a local run, Slurm, or Google Cloud Compute. Identification and masking of ambiguous
402 positions were conducted using SAMtools consensus (Li et al. 2009) (v1.17) after Minimap2
403 (default) (v.2.26) (Li 2018) or BWA (v.0.7.17) (alternative) mapping (Li and Durbin 2010)
404 (v.2.26). Different mapping approaches were tested (Supplementary Figures 7 and 8).
405 PlasFlow (Krawczyk et al. 2018) (v1.1.0) extracts chromosome contigs for downstream
406 analysis without plasmid sequences. R was utilized to plot sequence motifs (Figure 2B) with
407 ggseqlogo (Wagih 2017) and a violin chart comparing base frequencies per strand (Figure
408 2A) with ggplot2 (Wickham 2016).

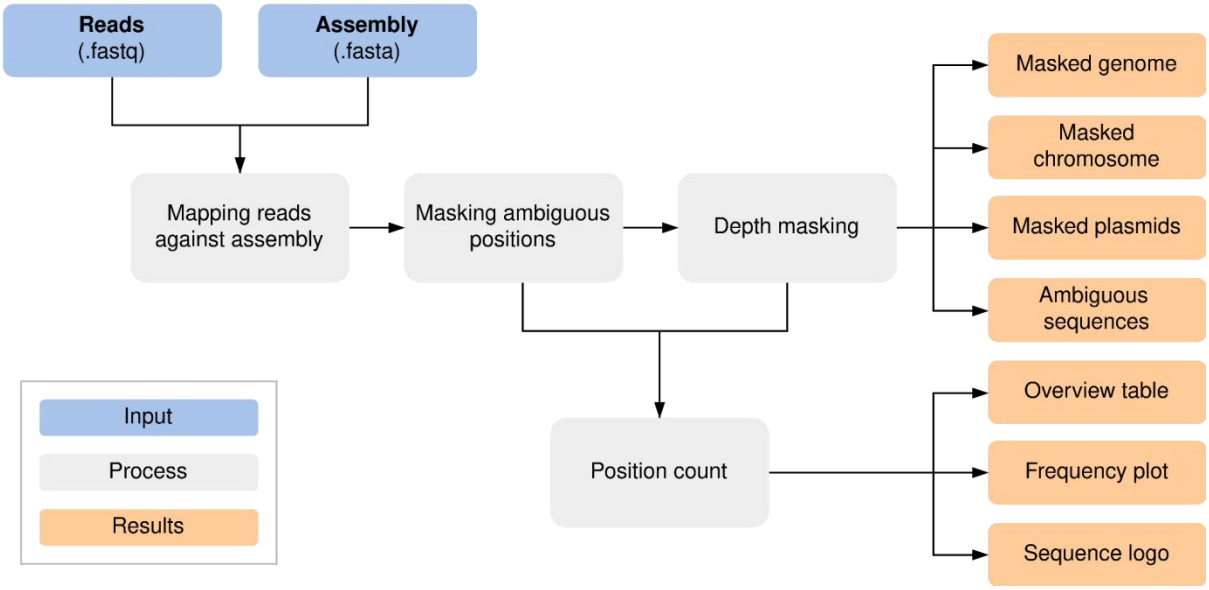

409

410 **Figure 4:** MPOA workflow to mask ambiguous and low coverage (0-10x sequencing depth)
411 positions in genome files. The workflow provides masked assemblies containing all contigs
412 and separate masked chromosomes and plasmid FASTA files. A FASTA file per sample is
413 also generated for each ambiguous position plus surrounding bases for further analysis
414 (github.com/replikation/MPOA; Supplementary Code 2).
415

Data access

The Workflow used in this study has been uploaded to GitHub (github.com/replikation/MPOA) and Supplementary_code_2.zip.

The Oxford Nanopore Technologies sequencing data generated in this study have been submitted to the NCBI BioProject database (https://www.ncbi.nlm.nih.gov/bioproject/?term=PRJNA1050168) under NCBI BioProject ID PRJNA1050168.

The Illumina sequencing data used in this study have been submitted to the NCBI BioProject database (https://www.ncbi.nlm.nih.gov/bioproject/?term=PRJNA742413) under NCBI BioProject ID PRJNA123456.

Competing interest statement

The authors declare no competing interests.

Acknowledgments

This work received financial support from the Ministry for Economics, Sciences and Digital Society of Thuringia (TMWWDG) under the framework of the Landesprogramm ProDigital (DigLeben-5575/10-9) and the Open Access Publication Fund of the Thueringer Universitaets- und Landesbibliothek Jena.

Authors' contributions

Sample collection and preparation: M.L., A.V., C.D; sequencing: M.L.; workflow development and testing: M.L. and C.B.; bioinformatic analysis: M.L. and C.B.; literature research: M.L.; writing first draft: M.L.; reviewing and editing manuscript: M.L., C.B., A.V., C.S, M.M., G.W.L, J.D.H., R.E, S.D.B., S.M., C.D and M.W.P.; supervision: C.B.; project administration: C.B.; cgMLST analysis: C.S.; funding acquisition: C.B.; providing genomes: M.L., S.D.B., S.M., A.V., G.W.L, J.D.H; All authors have read and agreed to the published version of the manuscript.

References

Abe R, Oyama F, Akeda Y, Nozaki M, Hatachi T, Okamoto Y, Yoshida H, Hamaguchi S, Tomono K, Matsumoto Y, et al. 2021. Hospital-wide outbreaks of carbapenem-resistant Enterobacteriaceae horizontally spread through a clonal plasmid harbouring blaIMP-1 in children's hospitals in Japan. *J Antimicrob Chemother* **76**: 3314–3317.

Argimón S, Abudahab K, Goater RJE, Fedosejev A, Bhai J, Glasner C, Feil EJ, Holden MTG, Yeats CA, Grundmann H, et al. 2016. Microreact: visualizing and sharing data for genomic epidemiology and phylogeography. *Microb Genom* **2**: e000093.

Bialek-Davenet S, Criscuolo A, Ailloud F, Passet V, Jones L, Delannoy-Vieillard A-S, Garin B, Le Hello S, Arlet G, Nicolas-Chanoine M-H, et al. 2014. Genomic Definition of Hypervirulent and Multidrug-Resistant *Klebsiella pneumoniae* Clonal Groups. *Emerg Infect Dis* **20**: 1812–1820.

Brandt C, Krautwurst S, Spott R, Lohde M, Jundzill M, Marquet M, Hölzer M. 2021. poreCov-An Easy to Use, Fast, and Robust Workflow for SARS-CoV-2 Genome Reconstruction via Nanopore Sequencing. *Front Genet* **12**: 711437.

Brandt C, Viehweger A, Singh A, Pletz MW, Wibberg D, Kalinowski J, Lerch S, Müller B, Makarewicz O. 2019. Assessing genetic diversity and similarity of 435 KPC-carrying plasmids. *Sci Rep* **9**: 11223.

Chewapreecha C, Holden MTG, Vehkala M, Välimäki N, Yang Z, Harris SR, Mather AE, Tuanyok A, De Smet B, Le Hello S, et al. 2017. Global and regional dissemination and evolution of Burkholderia pseudomallei. *Nat Microbiol* **2**: 16263.

Chiou C-S, Chen B-H, Wang Y-W, Kuo N-T, Chang C-H, Huang Y-T. 2023. Correcting modification-mediated errors in nanopore sequencing by nucleotide demodification and reference-based correction. *Commun Biol* **6**: 1215.

Di Tommaso P, Chatzou M, Floden EW, Barja PP, Palumbo E, Notredame C. 2017. Nextflow enables reproducible computational workflows. *Nat Biotechnol* **35**: 316–319.

Dohm JC, Peters P, Stralis-Pavese N, Himmelbauer H. 2020. Benchmarking of long-read correction methods. *NAR Genom Bioinform* **2**: lqaa037.

Eid J, Fehr A, Gray J, Luong K, Lyle J, Otto G, Peluso P, Rank D, Baybayan P, Bettman B, et al. 2009. Real-time DNA sequencing from single polymerase molecules. *Science* **323**: 133–138.

Gao Q, Lu S, Wang Y, He L, Wang M, Jia R, Chen S, Zhu D, Liu M, Zhao X, et al. 2023. Bacterial DNA methyltransferase: A key to the epigenetic world with lessons learned from proteobacteria. *Front Microbiol* **14**: 1129437.

Grohme MA, Schloissnig S, Rozanski A, Pippel M, Young GR, Winkler S, Brandl H, Henry I, Dahl A, Powell S, et al. 2018. The genome of Schmidtea mediterranea and the evolution of core cellular mechanisms. *Nature* **554**: 56–61.

Hadjadj L, Cassir N, Saïdani N, Hoffman C, Brouqui P, Astoul P, Rolain J-M, Baron SA. 2022. Outbreak of carbapenem-resistant enterobacteria in a thoracic-oncology unit through clonal and plasmid-mediated transmission of the bla OXA-48 gene in Southern France. *Front Cell Infect Microbiol* **12**: 1048516.

Hallgren MB, Overballe-Petersen S, Lund O, Hasman H, Clausen PTLC. 2021. MINTyper: an outbreak-detection method for accurate and rapid SNP typing of clonal clusters with noisy long reads. *Biology Methods and Protocols* **6**: bpab008.

Jünemann S, Sedlazeck FJ, Prior K, Albersmeier A, John U, Kalinowski J, Mellmann A, Goesmann A, von Haeseler A, Stoye J, et al. 2013. Updating benchtop sequencing performance comparison. *Nat Biotechnol* **31**: 294–296.

Kolmogorov M, Yuan J, Lin Y, Pevzner PA. 2019. Assembly of long, error-prone reads using repeat graphs. *Nat Biotechnol* **37**: 540–546.

Krawczyk PS, Lipinski L, Dziembowski A. 2018. PlasFlow: predicting plasmid sequences in metagenomic data using genome signatures. *Nucleic Acids Res* **46**: e35.

Leija-Salazar M, Sedlazeck FJ, Toffoli M, Mullin S, Mokretar K, Athanasopoulou M, Donald A, Sharma R, Hughes D, Schapira AHV, et al. 2019. Evaluation of the detection of *GBA*

494 missense mutations and other variants using the Oxford Nanopore MinION. *Molec*
495 *Gen & Gen Med* **7**: e564.
496 Leopold SR, Goering RV, Witten A, Harmsen D, Mellmann A. 2014. Bacterial Whole-
497 Genome Sequencing Revisited: Portable, Scalable, and Standardized Analysis for
498 Typing and Detection of Virulence and Antibiotic Resistance Genes ed. Y.-W. Tang.
499 *J Clin Microbiol* **52**: 2365–2370.
500 Lerminiaux NA, Cameron ADS. 2019. Horizontal transfer of antibiotic resistance genes in
501 clinical environments. *Can J Microbiol* **65**: 34–44.
502 Li H. 2018. Minimap2: pairwise alignment for nucleotide sequences. *Bioinformatics* **34**:
503 3094–3100.
504 Li H, Durbin R. 2010. Fast and accurate long-read alignment with Burrows–Wheeler
505 transform. *Bioinformatics* **26**: 589–595.
506 Li H, Handsaker B, Wysoker A, Fennell T, Ruan J, Homer N, Marth G, Abecasis G, Durbin R,
507 1000 Genome Project Data Processing Subgroup. 2009. The Sequence
508 Alignment/Map format and SAMtools. *Bioinformatics* **25**: 2078–2079.
509 Linde J, Brangsch H, Hölzer M, Thomas C, Elschner MC, Melzer F, Tomaso H. 2023.
510 Comparison of Illumina and Oxford Nanopore Technology for genome analysis of
511 Francisella tularensis, Bacillus anthracis, and Brucella suis. *BMC Genomics* **24**: 258.
512 Mellmann A, Bletz S, Böking T, Kipp F, Becker K, Schultes A, Prior K, Harmsen D. 2016.
513 Real-Time Genome Sequencing of Resistant Bacteria Provides Precision Infection
514 Control in an Institutional Setting ed. P. Bourbeau. *J Clin Microbiol* **54**: 2874–2881.
515 Miro E, Rossen JWA, Chlebowicz MA, Harmsen D, Brisse S, Passet V, Navarro F, Friedrich
516 AW, García-Cobos S. 2020. Core/Whole Genome Multilocus Sequence Typing and
517 Core Genome SNP-Based Typing of OXA-48-Producing Klebsiella pneumoniae
518 Clinical Isolates From Spain. *Front Microbiol* **10**: 2961.
519 Moura de Sousa J, Lourenço M, Gordo I. 2023. Horizontal gene transfer among host-
520 associated microbes. *Cell Host Microbe* **31**: 513–527.
521 Murray CJL, Ikuta KS, Sharara F, Swetschinski L, Robles Aguilar G, Gray A, Han C,
522 Bisignano C, Rao P, Wool E, et al. 2022. Global burden of bacterial antimicrobial
523 resistance in 2019: a systematic analysis. *The Lancet* **399**: 629–655.
524 Ni Y, Liu X, Simeneh ZM, Yang M, Li R. 2023. Benchmarking of Nanopore R10.4 and R9.4.1
525 flow cells in single-cell whole-genome amplification and whole-genome shotgun
526 sequencing. *Comput Struct Biotechnol J* **21**: 2352–2364.
527 Pletz MW, Wollny A, Dobermann U-H, Rödel J, Neubauer S, Stein C, Brandt C, Hartung A,
528 Mellmann A, Trommer S, et al. 2018. A Nosocomial Foodborne Outbreak of a VIM
529 Carbapenemase-Expressing Citrobacter freundii. *Clin Infect Dis* **67**: 58–64.
530 Price MN, Dehal PS, Arkin AP. 2009. FastTree: Computing Large Minimum Evolution Trees
531 with Profiles instead of a Distance Matrix. *Molecular Biology and Evolution* **26**: 1641–
532 1650.
533 Quinlan AR, Hall IM. 2010. BEDTools: a flexible suite of utilities for comparing genomic
534 features. *Bioinformatics* **26**: 841–842.
535 Sanderson ND, Kapel N, Rodger G, Webster H, Lipworth S, Street TL, Peto T, Crook D,
536 Stoesser N. 2023. Comparison of R9.4.1/Kit10 and R10/Kit12 Oxford Nanopore
537 flowcells and chemistries in bacterial genome reconstruction. *Microb Genom* **9**:
538 mgen000910.
539 Sivertsen A, Billström H, Melefors Ö, Liljequist BO, Wisell KT, Ullberg M, Özenci V,
540 Sundsfjord A, Hegstad K. 2014. A multicentre hospital outbreak in Sweden caused
541 by introduction of a vanB2 transposon into a stably maintained pRUM-plasmid in an
542 Enterococcus faecium ST192 clone. *PLoS One* **9**: e103274.
543 Spott R, Schleenvoigt BT, Edel B, W Pletz M, Brandt C. 2022. A Rare Case of Periprosthetic
544 Streptobacillosis - Rapid Identification via Nanopore Sequencing after Inconclusive
545 VITEK MS Results. *Arch Clin Med Case Rep* **06**.
546 Tourancheau A, Mead EA, Zhang X-S, Fang G. 2021. Discovering multiple types of DNA
547 methylation from bacteria and microbiome using nanopore sequencing. *Nat Methods*
548 **18**: 491–498.

549 Tyson JR, O'Neil NJ, Jain M, Olsen HE, Hieter P, Snutch TP. 2018. MinION-based long-read
550 sequencing and assembly extends the Caenorhabditis elegans reference genome.
551 *Genome Res* **28**: 266–274.
552 Viehweger A, Blumenscheit C, Lippmann N, Wyres KL, Brandt C, Hans JB, Hölzer M, Irber L,
553 Gatermann S, Lübbert C, et al. 2021. Context-aware genomic surveillance reveals
554 hidden transmission of a carbapenemase-producing Klebsiella pneumoniae. *Microb*
555 *Genom* **7**: 000741.
556 Wagih O. 2017. ggseqlogo: a versatile R package for drawing sequence logos.
557 *Bioinformatics* **33**: 3645–3647.
558 Wagner GE, Dabernig-Heinz J, Lipp M, Cabal A, Simantzik J, Kohl M, Scheiber M,
559 Lichtenegger S, Ehricht R, Leitner E, et al. 2023. Real-Time Nanopore Q20+
560 Sequencing Enables Extremely Fast and Accurate Core Genome MLST Typing and
561 Democratizes Access to High-Resolution Bacterial Pathogen Surveillance. *J Clin*
562 *Microbiol* **61**: e0163122.
563 Wang X, Yu D, Chen L. 2023. Antimicrobial resistance and mechanisms of epigenetic
564 regulation. *Front Cell Infect Microbiol* **13**: 1199646.
565 Wang Y, Zhao Y, Bollas A, Wang Y, Au KF. 2021. Nanopore sequencing technology,
566 bioinformatics and applications. *Nat Biotechnol* **39**: 1348–1365.
567 Wickham H. 2016. *ggplot2: Elegant Graphics for Data Analysis*. Springer-Verlag New York.
568 Wyres KL, Lam MMC, Holt KE. 2020. Population genomics of Klebsiella pneumoniae. *Nat*
569 *Rev Microbiol* **18**: 344–359.